Rev. Energ. Ren. : Journées de Thermique (2001) 151-158

Energy Characteristics and Response Behaviour of Enthalpy Wheels in Cold Regions

Y. Mercadier et P. Brousseau

Université de Sherbrooke, Département de Génie Mécanique, Sherbrooke, Québec, JI K 2R 1, Canada

Abstract - *Enthalpy Recovery Ventilators (ERV) have been developed to serve simultaneously three purposes: ventilation, heat recovery and humidity control. They have been used in hot climate in order to decrease cooling and dehumidification loads. They could be used in cold climate too in order to decrease heating and humidification loads. The main component of an ERV is the hygroscopic thermal wheel (HTW). The economics of the ERV will strongly depend on the effectiveness of the HTW.*

Measuring and predicting the simultaneous heat and mass transfer processes that prevail in hygroscopic thermal wheels is a challenging problem. The model developed rests on four mass conservation equations, two energy conservation equations and five basic constitutive relations. Boundary conditions for the conservation equations are set for this rotary co-ordinates and the system was solved using a finite-difference method with ADI scheme.

The foregoing model was validated with experimental data, and then used to highlight the effect of various design and operating parameters on the overall performance of the ERV. The tangential distributions of the temperature at the inlet and outlet of the wheel are shown and a set of measured data for the sensible, latent and total energy and effectiveness is compared with the corresponding simulation results.

Next, a large number of numerical simulations were performed in order to examine the effect of design and operating parameters on the performance of the hygroscopic thermal wheel. The four most influential parameters were found to be the two NTU numbers, the Cr number and the temperature difference number. Other parameters such as non-symmetric split, aspect ratio of the wheel, humidity ratio, carry-over factors were examined. It was found, however, that their effect on the effectiveness of the wheel was less important.

This is a first step in a research project aimed at the design of more advanced hygroscopic thermal wheels. A second step was to simulate the wheel behaviour under frosting conditions [8]. The third step will be the design of new and optimised wheel with, among the interesting avenues are wheels split into unequal sections, wheels with heterogeneous coatings of desiccant materials, complex matrix configurations, flow channels and hybrid wheels, i.e. a hygroscopic wheel coupled to a thermal non-rectangular wheel rotating at different speeds.

Keywords: Heat Recovery - Thermal wheel - Heat Mass transfer - Energy wheel.

1. INTRODUCTION

Over the last decade, the use of Recovery Ventilators has increased with the improvement in the insulation and airtightness of new constructions (ASHRAE Standard 62-1989).

The hygroscopic thermal wheel (HTW) (Fig. 1) usually consists of a porous rotating cylindrical wheel made of an impermeable, metallic or plastic support and a coating or impregnated desiccant material. The support and the desiccant material form the matrix. The matrix is divided in two sections, i.e., the adsorption section and the regeneration (desorption) section.

For heating and humidifying applications (winter conditions), heat and moisture are transferred from the hotter and moister exhaust air stream from the building to the adsorption section. In the regeneration section, the stored heat and moisture are transferred to the cooler and dryer fresh air stream from outside. The system can be inverted to provide the building with cooled and dehumidified fresh air (summer conditions).

Predicting the simultaneous heat and mass transfer processes that prevail in periodic HTW has attracted growing research attention over the last ten years. Coppage and London [1] appear to be the firsts who evaluated successfully the sensible efficiency of industrial periodic regenerators, including thermal wheels. By coupling two separate hot and cold counterblow heat exchangers, they were able to simulate the whole periodic system with a modified C-NTU method. This approach was also adopted by Shoukri [2] and by Shah [3] for modelling non-desiccant rotating matrices.

Banks et al. [4] were the first to consider mass transfer within the regenerator. They developed a non-linear analogy method where performance predictions involves the evaluation of combined potentials that drive heat and mass transfer for each of the two superimposed regenerators.

Based on the previous approach Maclaine-Cross and Banks [5] developed what is referred as the "Wave theory of heat transfer" for regenerators where the heat and mass transfer relations become first order non- linear wave equations.

More recently, Zheng and Worek [6] proposed a one-dimensional transient flow model of a rotary dehumidifier. Relying on the usual assumptions, the model solves the mass and energy equations for a

representative channel in the regenerator. Good approximation of the system performance has been obtained considering the fact that the effects of axial heat and mass diffusion have been neglected.

The objective of this paper is to remedy these limitations. A new approach is used to derive the three-dimensional heat and mass transfer equations for an hygroscopic thermal wheel composed of any type of channel configuration. The conservation equations are then implemented in a numerical scheme and the resulting model is validated with experimental data. Finally, the effect of the most influential parameters on the overall performance of the hygroscopic thermal wheel is examined.

2. PHYSICAL MODEL AND NUMERICAL PROCEDURE

The modelling of the hygroscopic thermal wheel rests on the following assumptions :

1. The matrix consists of a homogeneous porous medium of constant porosity
2. The thermophysical properties of the dry matrix are constant
3. Pressure drops through the matrix are small with respect to the total pressure and, as a result, are neglected
4. The moist air stream is incompressible
5. The air stream enters the matrix with uniform and constant velocity
6. Leakage and carry over between the two air streams are neglected
7. Heat conduction and mass diffusion in the air stream are negligible with respect to convection
8. Energy associated with pressure variations and viscous dissipation are neglected
9. The matrix and the liquid water in the desiccant are in thermal equilibrium as well as the dry air and the water vapour.

A schematic of the hygroscopic thermal wheel is shown in Fig. 1. The wheel has an outer diameter D and an inner diameter d and a length L.

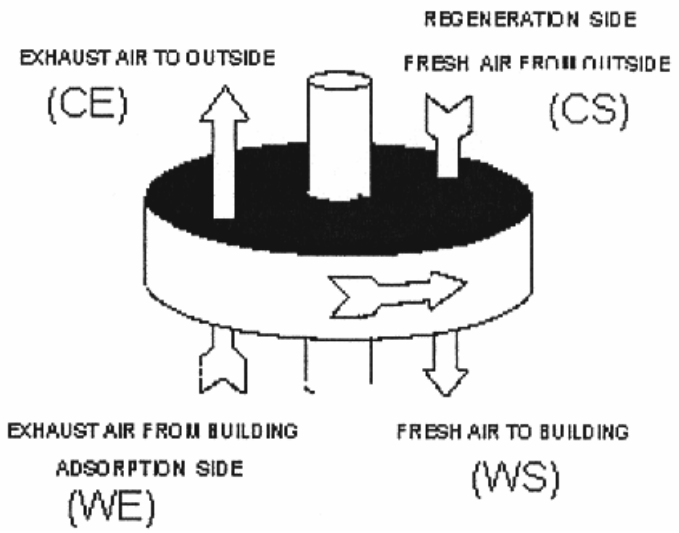

Fig. 1

Subject to the foregoing assumptions, the conservation equations for mass and energy will be derived for a finite control volume inside the wheel. The representative elementary volume encompasses the four constituents, that is the solid matrix (M), the dry air (a), the water vapour (v) and the liquid sorbate (l).

The overall and specific porosities of the wheel are defined as :

$$\varepsilon = \frac{V_a}{V} = 1 - \frac{V_M}{V} \quad , \quad \varepsilon_i = \frac{dV_i}{dV} \equiv \frac{dA_i}{dA} \quad i = M, a, v, l \qquad (1)$$

Conservation equation

A constituent density is defined as $\rho_i = \frac{m_i}{V_i}$ and its averaged value is $\overline{\rho}_i = \frac{m_i}{V} = \varepsilon_i \rho_i$. Thus the overall density of the wheel can be stated as $\rho = \sum \overline{\rho}_i$, and $\rho \, dV = \sum \rho_i \, dV_i$, where $\overline{J}_i = \varepsilon_i J_i$ and $\overline{r}_i = \varepsilon_i r_i$ are the averaged properties. Every constituents must be conserved, and equation (2) yields :

$$\frac{\partial \bar{\rho}_i}{\partial t} + \nabla . \bar{J}_i = \bar{r}_i \qquad i = M, a, v, l \tag{2}$$

The energy conservation equation for all the constituents of the wheel may be written in terms of the enthalpy h and the heat generation **Q**. It includes the effects of convective heat transfer that occurs when the constituents are taken separately.

$$\sum \bar{\rho} \frac{\partial h_i}{\partial t} + \sum \bar{J}_i . \nabla h_i = \sum \bar{Q}_i + \sum \nabla . \bar{q}_i - \sum \bar{r}_i . h_i \tag{3}$$

Constitutive equations

In order to determine the final form of the mass and energy conservation equations, it is necessary to define explicitly the mass flux (**J**), the mass generation (**r**), the heat generation (**Q**) and the heat diffusion (**q**). The mass flux comprises two terms : the advection term and the diffusion term i.e.,

$$J = J_{adv} + J_{dif} \tag{4}$$

where $\mathbf{J}_{adv} = \rho v$ and $\mathbf{J}_{dif}$ is given by Fick's law.

The only phase change that may occur in the system is between liquid water and water vapour. Thus, the mass generation term may be modelled as :

$$\bar{r}_i = \pm \varepsilon_i h_m (\rho_v - \rho_s) \frac{A}{V_i} \tag{5}$$

where h_m is the mass transfer coefficient and ρ_s is the density of the water vapour at the surface of the matrix. ρ_s depends on the type of desiccant used and is given by the adsorption isotherm. The ± sign depends on the constituent considered. It is **-** for the vapour and **+** for the liquid sorbat. The heat generation term (the jump condition) is modelled as :

$$\bar{Q}_i = \pm \varepsilon_i h (T_a - T_M) \frac{A_s}{V_i} \tag{6}$$

where h is there the heat transfer coefficient between the moist air and the wet matrix. Once again, the ± sign in equation (6) depends on the constituent considered. It is **-** for the moist air and **+** for the wet matrix.

The heat diffusion term is given by Fourier's law i.e.,

$$Q_i = -k_i \nabla T_i \tag{7}$$

Closure law

An additional relation is needed to close the system of equations which is called the "adsorption isotherm". This expression may be stated as :

$$\rho_s = fct(\rho_l , T_M , T_a) \tag{8}$$

ρ_s can be derived from the Clausius-Clapeyron equation but it is generally given in terms of an empirical function. For silica gel, e.g., eq. (8) becomes :

$$\Phi = (2.112\,W)^{h^*} (29.91\,P_{ws})^{h^*-1}, \text{ where } h^* = 1 + 0.2843\exp(-10.28\,W) \tag{9}$$

Since $\bar{\rho}_a$ and $\bar{\rho}_M$ are assumed constant, it is possible to abridge the writing by defining two new variables: the humidity ratio of the moist air (ω) and the moisture content in the desiccant material (W)

$$\omega = \frac{m_v}{m_a} = \frac{\bar{\rho}_v}{\rho_a} \qquad W = \frac{m_l}{m_d} = \frac{m_l}{f\, m_M} = \frac{\bar{\rho}_l}{f\, \bar{\rho}_M} \tag{10}$$

m_d and f are the mass and the mass fraction of desiccant in the matrix respectively.

With respect to assumption 9, only two energy conservation equations are needed to describe the system. If T_a and T_M represent respectively the temperature of the moist air and of the wet matrix, the final conservation equations are :

$$\frac{\partial \varpi}{\partial t} + v.\nabla \omega = - h_m (\omega - \omega_s) \frac{A_s}{V_v} \tag{11}$$

$$\frac{\partial W}{\partial t} = \mu h_m (\omega - \omega_s) \frac{A_s}{V_v} \qquad \text{where} \quad \mu = \frac{\bar{\rho}_a}{f \bar{\rho}_M} \tag{12}$$

$$\frac{\partial T_a}{\partial t} + v.\nabla T_a = -\frac{h}{\bar{\rho}_a (c_a + \omega c_v)} (T_a - T_M) \frac{A_s}{V} + \mu \frac{h_m}{(c_a + f W_{Cl})} (\omega - \omega_s) \frac{A_s}{V_v} h_v \tag{13}$$

$$\frac{\partial T_M}{\partial t} = -\frac{h}{\bar{\rho}_M (c_M + f W_{cl})} (T_a - T_M) \frac{A_s}{V} + \mu \frac{h_m}{(c_a + f W_{cl})} (\omega - \omega_s) \frac{A_s}{V_v} h_l \tag{14}$$

Boundary conditions

At the circumferential limit of the wheel, r = D/2 and r = D/2 and 0 < z < L

$$\frac{\partial \omega}{\partial r} = \frac{\partial W}{\partial r} = \frac{\partial T_a}{\partial r} = \frac{\partial T_M}{\partial r} = 0 \tag{15}$$

At the inlet of the regeneration section, $z = 0$, $d \le 2r \le D$ and $\Omega t \le \theta \le \Omega t + \pi$

$$\omega = \omega_{reg,in} \quad ; \quad \frac{\partial W}{\partial z} = 0 \quad ; \quad \frac{\partial T_M}{\partial z} = 0 \quad ; \quad T_a = T_{a,reg,in} \tag{16}$$

At the inlet of the adsorption section, $z = L$, $d \le 2r \le D$ and $\Omega t + \pi \le \theta \le \Omega t + 2\pi$

$$\omega = \omega_{reg,in} \quad ; \quad \frac{\partial W}{\partial z} = 0 \quad ; \quad \frac{\partial T_M}{\partial z} = 0 \quad ; \quad T_a = T_{a,ads,in} \tag{17}$$

and at the outlet of the wheel,

$$\frac{\partial \omega}{\partial z} = \frac{\partial W}{\partial z} = \frac{\partial T_a}{\partial z} = \frac{\partial T_M}{\partial z} = 0 \tag{18}$$

Equations (11)-(14) may be cast in the following standard form : $\frac{\partial \phi}{\partial t} + v.\nabla \phi = S_\phi$, where ϕ is the general dependent variable which stands for ω, W, T_a or T_M .

S_ϕ is a source term that may be linearized as $S_\phi = S_c + S_p \phi$. The equation system is solved using a finite-difference method with a ADI scheme. The numerical implementation of these schemes are fully discussed in [7]. The convergence of the method is declared when the largest residual for all difference equations is smaller than 10^{-3}. Moreover, the overall mass balance and energy balance at a given time step must be :

$$\frac{\text{Rate of accumulation of mass} - \text{Mass in} + \text{Mass out}}{\text{Mass in}} < 0.01$$

$$\frac{\text{Rate of accumulation of energy} - \text{Energy in} + \text{Energy out} \pm \text{Energy generated}}{\text{Energy in}} < 0.01$$

3. RESULTS AND DISCUSSION

The foregoing model was first examined in a simple one-dimensional case and next validated with experimental data. It was then employed to highlight the effect of various design and operating parameters on the overall performance of the ERV.

The objective of this section is to summarise these findings. The present model was compared to the one of Zheng and Worek [8] for the heat and mass transfer in a rectangular channel (Fig. 2).

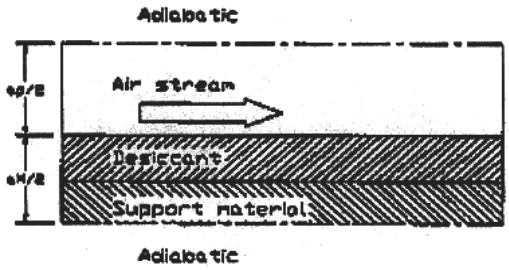

Fig. 2

Assuming that the accumulation terms in the air stream equations are negligible and expressing the temperature in terms of enthalpy, equations (11)-(14) for the one-dimensional flow depicted in Fig. 2 become :

$$\frac{\partial \omega}{\partial x} = -\frac{2K}{a_p \rho_a \cup_a}(\omega - \omega_s) \tag{19}$$

$$\frac{\partial W}{\partial t} = \frac{2K}{a_M \rho_M f}(\omega - \omega_s) \tag{20}$$

$$\frac{\partial h_a}{\partial x} = -\frac{2h}{a_p \rho_a \cup_a}(T_a - T_M) + \frac{2k}{a_p \rho_a \cup_a}(\omega - \omega_s) h_v \tag{21}$$

$$\frac{\partial h_m}{\partial t} = -\frac{2h}{a_M \rho_M}(T_a - T_M) - \frac{2k}{a_M \rho_M f}(\omega - \omega_s) h_l \tag{22}$$

It appears now that the energy term associated with the water phase change (last term, equations (21) and (22) is different from [8]. This term is not a jump condition but, indeed, results from the definition of the phase change rate. The summation of (21) and (22) implies that, for an entire representative elementary volume, the variation of the energy in the air stream and the energy accumulation in the matrix are equal to the evaporation (condensation) energy associated with the water phase change.

The proposed model may handle, equally well, more complex matrix configurations made, for example, of textile fibbers or glass fibbers with flow channels of different shapes. This information is provided to the model via the geometrical properties, i.e., the surface area density (A_s/V) and the porosity (ε) of the matrix.

To illustrate the model predictive capabilities, it was confronted to experimental data obtained from a commercial enthalpy recovery ventilator. A layout of the experimental set- up is depicted in Fig. 3. The major components of the system are the enthalpy recovery ventilator, the climatic chamber, the ventilation pipes and the data acquisition system. Operating conditions may range from -30 °C to 40 °C and air flow rates up to 80 l/s. The mean inlet and outlet dry bulb and dew point temperatures are measured with thermocouples.

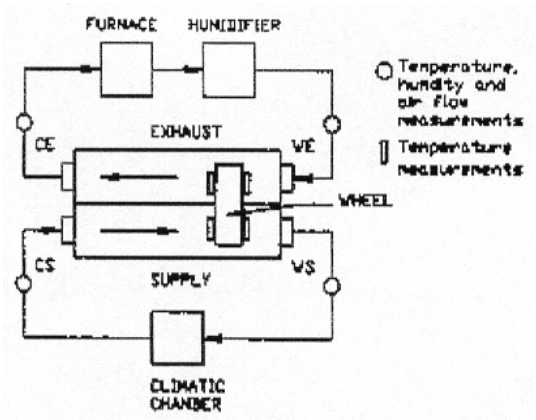

Fig. 3

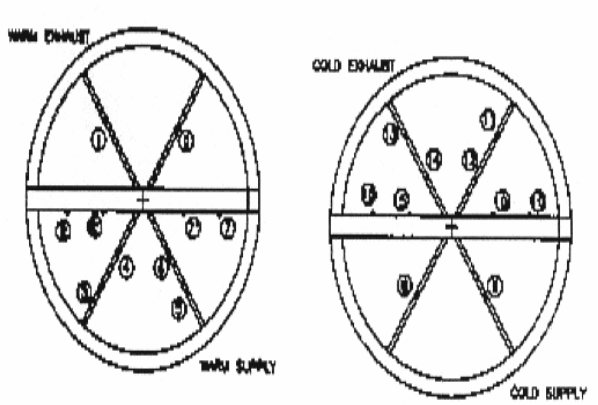

Fig. 4

The temperatures of the air streams passing through the HTW are measured by an array of 20 thermocouples (Fig. 4) directly positioned at inlet and outlet faces of the wheel.

Experimental errors were estimated according to the ASMIE and the ANSI standards. The experiments were conducted with a HTW of D = 30.5 cm and L = 9.5 cm. The rotational speed of the wheel was kept constant at 16 rpm.

Seven experiments, were carried out that cover a large range of cold supply (CS) temperature and warm exhaust (WE) humidity normally encountered for house ventilation in cold regions.

The (CS) humidity was kept at 0.233 g/kg as the (WE) temperature at 22 °C.

A comparison between the experimentally determined and predicted outlet temperature and absolute humidity for the warm supply and the cold exhaust is provided in Figs 5 - 6.

The numerical simulations were carried out with a grid size of 38 x 6 x 32 non uniformly distributed nodes in the θ-r-z direction respectively. The time step was chosen so as to match the rotational speed of the wheel with the mesh size in the θ direction.

Figs 5 - 6 reveal that the numerical predictions are, in general, in very good agreement with the experimental results. The slight discrepancy between the predicted and measured humilities may be attributed to the imprecise model inputs, material properties and heat and mass transfer coefficients. The tangential distributions of the temperature at the inlet and outlet of the wheel are exemplified in Fig 7. Once again, the numerical predictions agree well with the experimental data. The disagreement between the predicted and measured (CE) temperatures for angles between 180 ° and 225 ° is due to the cross leakage, between (CS) and (CE) air streams.

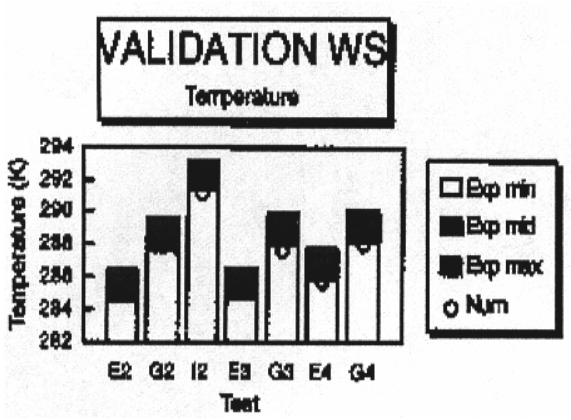

Fig. 5

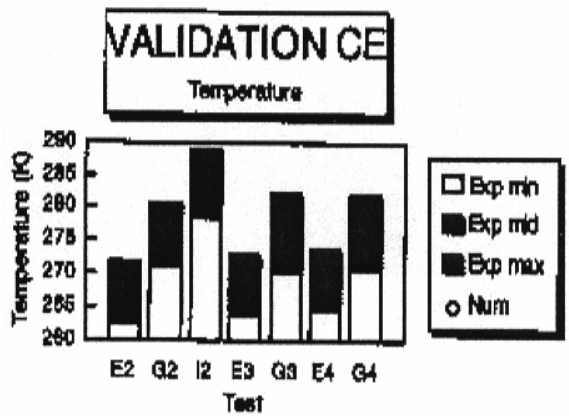

Fig. 6

Next, a series of more than 400 numerical simulations were performed in order to examine the effect of a number of design and operating parameters on the performance of the hygroscopic thermal wheel. The four most influential parameters were found to be the NTU Fig. 8 and C_r Fig. 9 numbers and the temperature difference parameter, T^*, defined as. The sensible effectiveness of the wheel is defined as

$$T^* = \frac{1}{2}\frac{(T_{CS} + T_{WE})}{|T_{WE} - T_{CS}|} \qquad \text{and} \qquad \varepsilon = \frac{C_c\,(T_{WS} - T_{CS})}{C_{min}\,(T_{WE} - T_{CS})} = \frac{C_h\,(T_{WE} - T_{CE})}{C_{min}\,(T_{WE} - T_{CS})} \qquad (24)$$

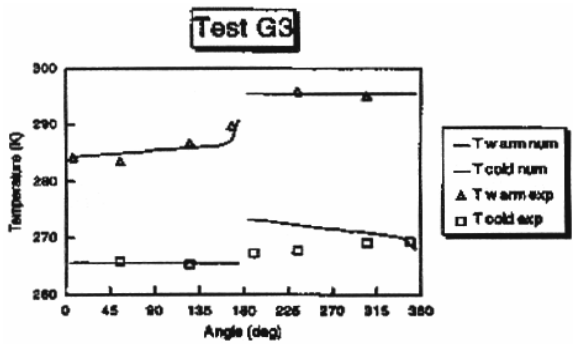

Fig. 7

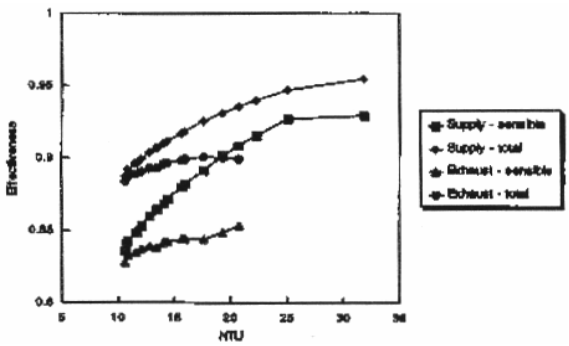

Fig. 8

The total effectiveness follows the same definition by replacing the temperature by the enthalpy and by omitting the specific heat in the heat capacity rates. It is seen from Fig. 8 that the supply side NTU plays a more important role in determining the overall performance of the wheel than does the exhaust side NTU number. This is an indication that the adsorption side is probably over designed. In the present design, the wheel is split into two equal sections each spanning 180°. One may then envisage the possibility of increasing the flow passage of the supply air stream (180° + Δ) by decreasing in the same proportion (180° - Δ) the flow passage of the exhaust air stream. In doing so, the adsorption side pressure drop would however increase.

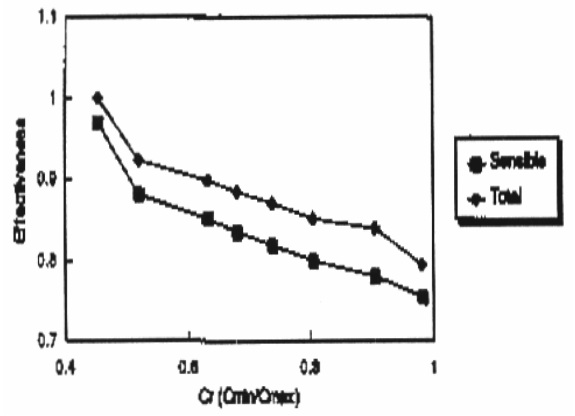

Fig. 9

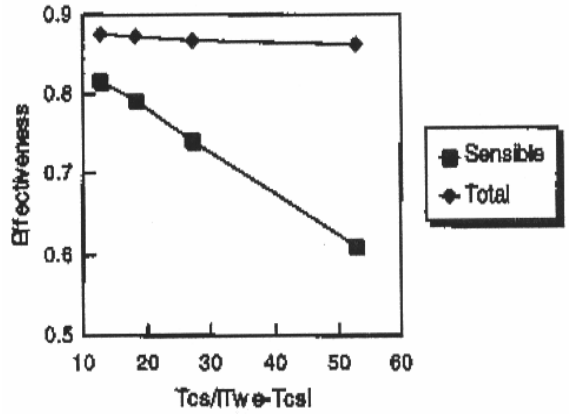

Fig. 10

Figure 9 illustrates the effect of the C, number on the effectiveness of the wheel. These results are consistent with the theory of heat exchangers. Unfortunately, for house ventilation, the supply air flow rate is, in general, matched by the exhaust air flow rate, i.e., Cr ≈ 1 resulting in the lowest effectiveness. Fig. 10 shows the variation of the sensible and of the total effectiveness as a function of the temperature difference parameter. This figure reveals that the sensible effectiveness is strongly influenced by this parameter. For example, an increase of 15 °C of the cold supply temperature will result in a decrease of nearly 22 % in the sensible effectiveness. On the other hand, the total effectiveness is nearly independent of the temperature difference. The reason is that the hydric effectiveness increases when the difference between T_{CS} and T_{WE} decreases. Other parameters such as the aspect ratio of the wheel (A_C/A_S), the carry- over factors CO_C and CO_h, two unnamed parameters $\Omega\sqrt{\frac{A_S}{|T_{WE} - T_{CS}|}}$ and $\frac{A^{3/2}}{V}$ and the humidity ratio $\frac{\omega_{CS}}{|\omega_{WE} - \omega_{CS}|}$ were examined. It was found, however, that their effect on the effectiveness of the wheel was less important.

4. CONCLUSION

A three-dimensional model for the heat and mass transfer in enthalpy (hygroscopic thermal) wheels was developed. The model rests on four mass conservation equations, two energy conservation equations and five basic constitutive relations. The model was compared to another analytical model and validated with experimental data obtained with a commercial wheel. Numerical simulations have revealed that the performance of the wheel is strongly dependent on the NTU and C, numbers and on the temperature difference parameter. On the other hand, the effect of the aspect ratio of the wheel, of the humidity factor and of the carry over factors for

the cold and the warm side was found to be less influential. The sensible and the total effectiveness of the wheel were correlated in terms of the main design and operating parameters.

This paper was a first step in a research project aimed at the design of more advanced hygroscopic thermal wheels. In the near future, the fully three- dimensional capabilities of the model will be exploited in order to increase the performance of the wheels. Among the interesting avenues are wheels split into unequal sections, wheels with heterogeneous coatings of desiccant materials, complex matrix configurations, non- rectangular flow channels and hybrid wheels, i.e. a hygroscopic wheel coupled to a thermal wheel rotating at different speeds.

ACKNOWLEDGEMENTS

The authors would like to thank the Natural Sciences and Engineering Research Council of Canada for their financier support.

REFERENCES

[1] J.E. Coppage and A.L. London, Transactions of the ASME, New-York, ASME, Vol. 75, pp. 779-787, 1953.
[2] M. Shoukri, ASME Paper, New-York, ASME, December 1979.
[3] R.K. Shah, [1980], Conf. NATO Adv. Study Inst.-Heat Exchangers : Thermal-Hydraulic Fund. and Design, New-York, McGraw-Hill Book Co., pp. 721-764, 1981.
[4] P.J. Banks, D.J. Close and I.L. Maclaine-Cross, Paper CT 3.1, Heat Transfer , Proceedings of the Fourth International Conference, Versaille, Vol. Vfi, pp. 1-10, September 1970.
[5] I.L. MacLaine-Cross and P.J. Banks, International Journal of Heat and Mass Transfer, UK, Pergamon Press, Vol. 15, pp. 1225-1242, 1972.
[6] W. Zheng and W.M. Worek, Numerical Heat Transfer; Part A, N°l, 23, N°2, pp. 211-232, March 1993.
[7] P. Brousseau, PhD Thesis, Unversity of Sherbrooke, Canada, 1999.
[8] S. Bilodeau, P. Brousseau, M. Lacroix and Y. Mercadier, International Journal of Heat and Mass Transfer, N°42, pp 2605-2619, 1999.